Biosensors

DOI: 10.1002/anie.200703881

# Combining Resonant Piezoelectric Micromembranes with Molecularly Imprinted Polymers**

*Cédric Ayela,* Fanny Vandevelde, Denis Lagrange, Karsten Haupt,* and Liviu Nicu*

Environmental analysis deals with both instantaneous characterization and long-term monitoring of media like water, soil, and air, to gather information on the quality of the environment and detect pollution and degradation.[1,2] It commonly relies on biological, biochemical, or chemical assays or on (bio)sensors. Biosensors are composed of a sensitive layer, such as a layer of enzyme or antibody, and a transducer. However, the short shelf-life, low stability, and environmental intolerance of biomacromolecules sometimes compromise their usefulness in environmental field analysis and unattended monitoring. Molecularly imprinted polymers (MIPs) are synthetic receptors that can address some of these issues.[3] MIPs are characterized by their capability of binding target molecules with similar affinities and selectivities to those of antibodies, enzymes, or hormone receptors. They also offer a greater stability and better engineering possibilities than biomacromolecules when interfaced with transducers. For example, we recently succeeded in directly patterning MIP microdot arrays on gold surfaces by using silicon microcantilever arrays.[4] However, the combination of MIP arrays with sensors in a suitable format remains a challenge. Since the pioneering works of Dickert et al.[5] and others,[6] the combination of acoustic sensors and other label-free transducers with MIPs has attracted much attention,[7] although these techniques still suffer from their lack of multiplexing capabilities and integration. Although MIP multisensors and sensor arrays were predicted some time ago,[8] only one example, an SPR chip, has been reported that can be qualified as a MIP-based, although not integrated, multisensor.[9]

We believe that silicon microfabrication technology might close the aforementioned gap, since micromachining techniques allow the production of sensor arrays with multiplexing capabilities and high integration. In this context, microelectromechanical systems (MEMS) as transducers coupled to a sensitive layer have great potential.[10] The use of microcantilevers for biosensors was reported,[11] although their individual functionalization remains a challenge because their low stiffness limits the usable interfacing techniques. Silicon micromembranes are another alternative. They possess a better rigidity and show reduced damping when working in dynamic mode in liquid media.[12]

Herein, we show the first experimental proof of concept of the combination of resonant MEMS with MIPs. We report the fabrication, characterization, and use of a sensor composed of silicon-based micromembranes carrying piezoelectric thin films for integrated excitation–detection purposes (Figure 1 a), the surfaces of which are coated with MIPs for the detection of target analytes. In this preliminary work, a MIP selective for the herbicide 2,4-dichlorophenoxyacetic acid (2,4-D) and a nonimprinted control polymer (NIP) were used and their interfacing with the sensor membranes was studied.

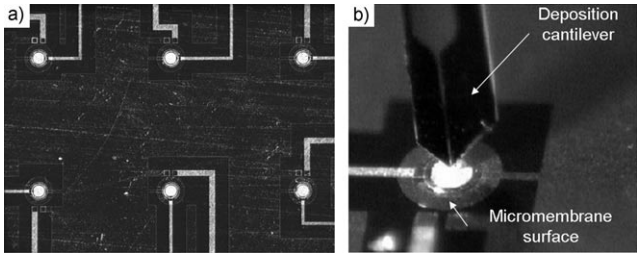


***Figure 1.*** Images of a) a matrix of piezoelectric micromembranes with a global radius of 100 μm and b) a cantilever loaded with MIP precursor solution during deposition onto a micromembrane.

The polymers were based on trimethylolpropane trimethacrylate (TRIM) as the cross-linker and 4-vinylpyridine (4-VP) as the functional monomer. Diglyme was used as the porogenic solvent, which contained 1% poly(vinyl acetate) (PVAc) as a coporogen. The micromembrane arrays were individually coated with MIPs by using a cantilever array-based deposition tool (Figure 1 b).[4] Measurement of the resonance frequency of the structures before and after deposition ($\Delta f_{\text{deposition}}$) of the precursor solutions revealed a significant decrease, which transduces the mass increase on the sensors surface and allows determination of the deposited volume ($V_{\text{MIP}}$) through the mass sensitivity ($S_{\text{membrane}}$) of the structures and the density of the prepolymerized mixture (referred to as $\rho_{\text{MIP}}$). Indeed, for mass-based sensors, mass variations can be linearly related to frequency shifts through the mass sensitivity, $\Delta m = S_{\text{membrane}} \times \Delta f$, as established by a theoretical model[13] and experimentally validated. The values

[*] C. Ayela, D. Lagrange, Dr. L. Nicu
NanoBioSystems Department
Laboratory for Analysis and Architecture of Systems-CNRS
University of Toulouse, 31077 Toulouse (France)
Fax: (+33) 5-61-33-62-08
E-mail: cayela@laas.fr

F. Vandevelde, Prof. K. Haupt
Compiègne University of Technology
CNRS UMR 6022
BP 20529, 60205 Compiègne Cedex (France)
Fax: (+33) 3-44-20-39-10
E-mail: karsten.haupt@utc.fr

[**] We thank Caroline Soyer and Denis Remiens from IEMN-CNRS for providing us with PZT layers. We also thank Hélène Lalo for her valuable help in the AFM experiments.

Supporting information for this article is available on the WWW under http://www.angewandte.org or from the author.

ranged from 1.7 to 2.5 Hz pg$^{-1}$ and were dependent on the initial value of the resonance frequency. The deposited volumes were calculated by using Equation (1).

$$V_{MIP} = \frac{\Delta f_{deposition}}{S_{membrane}\,\rho_{MIP}} \quad (1)$$

The values ranged from 8.4 to 68.1 pL. In this equation, the frequency shift is assumed to be due to the density of the prepolymerized mixture and the viscosity effects are ignored.

The droplets were immediately polymerized under UV light in an $N_2$-saturated atmosphere. An electronic setup allowed the multiplexed real-time tracking of the resonance frequency of the micromembranes for the dynamic characterization of the MIP during polymerization. When the UV light was turned on, the resonance frequency increased dramatically during the first five minutes; this was followed by a second phase with smaller variation of the resonance frequency before a maximum value was reached (Figure 2).

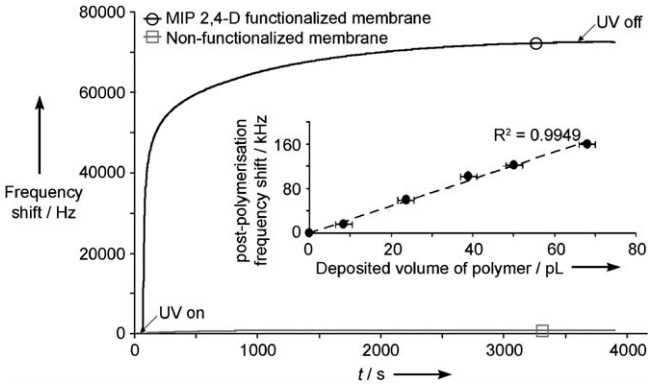


***Figure 2.*** Real-time monitoring of the resonance frequency of micromembranes during UV irradiation of deposited MIP precursor solution. Inset: Resonance-frequency variation after polymerization for different deposited quantities of 2,4-D MIP.

Two effects might have induced this frequency increase: a mass decrease or a stiffness increase. A mass decrease is unlikely though, as low-vapor-pressure solvents and monomers were used at a temperature not exceeding 306 K during polymerization. The resonance-frequency increase seemed rather to reflect the strengthening of the layer by cross-linking polymerization. Real-time monitoring of the polymerization process thus allowed determination of the minimum polymerization time. The measured frequency shift after droplet deposition and polymerization showed a linear dependency on the deposited volume of the precursor solution (Figure 2). The relevance of these results was confirmed by the negligible frequency variation for nonfunctionalized neighboring micromembranes used as controls.

Removal and rebinding of the template 2,4-D was studied in dip-and-dry experiments, where the resonance frequency was measured after each washing and incubation cycle. A first wash to remove the template resulted in a large frequency increase of the micromembrane bearing the 2,4-D MIP, while much smaller effects were observed on the NIP membrane (Figure 3). After incubation in a 2,4-D solution, the resonance frequency decreased on the MIP membrane, whereas the NIP membrane again showed a very small variation. One could

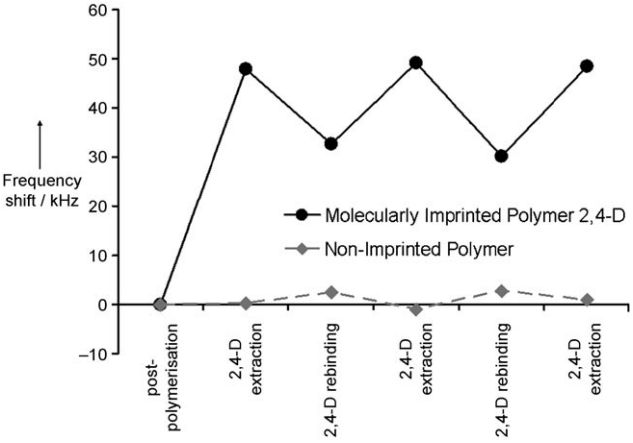


***Figure 3.*** Reproducibility of resonance-frequency measurements for successive 2,4-D removal and rebinding cycles. A 10 μM solution of 2,4-D in 20 mM phosphate buffer (pH 7) was used during the rebinding steps, while a mixture of acetic acid and ethanol (1:10) was used for the template removal.

expect the resonance frequency after incubation to return to the postpolymerization value; however, this was not the case, which indicated that the yield of binding sites during imprinting was less than 100%. Subsequent cycles showed good reproducibility of the frequency changes. The standard deviation for the MIP membrane was 1.7 kHz (less than 0.3% of the postpolymerization value) after four washing and incubation cycles.

The washing and incubation cycles were then repeated on different 2,4-D MIP functionalized micromembranes. The resonance-frequency shift after the incubation step showed a dependency on the quantity of deposited MIP (Figure 4). Since the quantity of the 2,4-D template increased with the volume of MIP, the absolute frequency shift between the washing and incubation cycles also increased. However, the

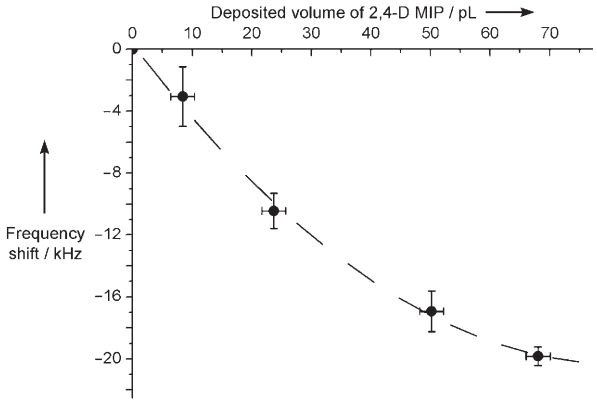


***Figure 4.*** Influence of the deposited quantity of MIP on the resonance frequency of the micromembranes after rebinding of 2,4-D in 20 mM phosphate buffer (pH 7).

  

frequency shift seemed to tend toward a maximum value, which indicated better surface accessibility than volume accessibility of the MIP and thus mass-transfer limitations, despite the use of a polymer coporogen that generated porosity in the MIP.

Another important parameter is the cross-reactivity of the 2,4-D MIP with structurally closely related compounds. Initial reports on 2,4-D MIPs had shown, by radioligand binding, a relatively low cross-reactivity of related compounds,[14] which indicated good selectivity of the synthetic receptor. We performed binding experiments by incubating the 2,4-D MIP micromembranes in 2,4-D and phenoxyacetic acid (POAc; 2,4-D lacking the two chlorine atoms on the aromatic ring) at concentrations up to 100 μM (Figure 5). With 2,4-D, a

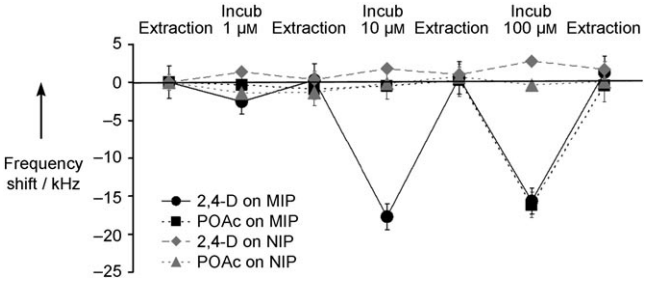


***Figure 5.*** Detection of the rebinding of 2,4-D and POAc at increasing concentrations on a 2,4-D MIP and a NIP. 2,4-D and POAc were dissolved in 20 mM phosphate buffer (pH 7), while a mixture of acetic acid and ethanol (1:10) was used for the washing steps.

reproducible frequency shift (−16.5 kHz) was observed at the 10 μM concentration, while no variation was measured on the NIP micromembrane. A concentration of 100 μM did not result in a further increase in frequency shift; the slightly lower mean value (−15.5 kHz) is still within the experimental error of that at 10 μM and is probably due to the dip-and-dry format of the measurements. With POAc, a significant variation of the frequency was obtained only at the 100 μM concentration. The ten times higher concentration of POAc (compared to 2,4-D) required to generate the same frequency shift is in agreement with the literature[15] where similar data were obtained for a 2,4-D MIP studied by evanescent-wave IR spectroscopy.

To verify that the different behaviors of the 2,4-D MIP and the NIP were not simply due to a difference in morphology, we used contact-mode atomic force microscopy to characterize the polymer surfaces (Figure 6). The scans showed that addition of 1% PVAc to the porogenic solvent resulted in the formation of visible pores on both the MIP and the NIP. This had already been shown in earlier reports on thin MIP structures.[4,16] The size, density, and distribution of the pores are clearly similar on the MIP and the NIP. The pore sizes range from 200 to 400 nm in diameter, with a few pores of 100 nm in diameter; the values confirm the comparable physical morphologies of the 2,4-D imprinted polymer and the nonimprinted control.

In summary, the possible use as biosensors of piezoelectric circular micromembrane arrays combined with molecularly

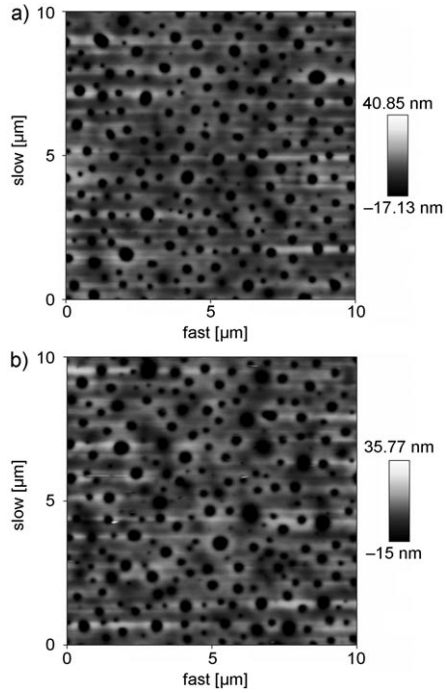


***Figure 6.*** Atomic force microscopy images (10×10 μm², contact mode) of a) the 2,4-D MIP and b) the NIP with addition of 1% PVAc to the porogenic solvent.

imprinted polymers was investigated. This study allowed us to take advantage of the MEMS resonating structures to follow the polymerization in situ, as well as to monitor the subsequent processing steps of the MIPs. We also demonstrated the possibility of measuring several micromembranes in parallel and thus the potential use of the device as a multisensor. The capability of selectively and reproductively detecting analyte molecules through washing and incubation cycles was demonstrated. The stability of MIPs combined with MEMS as acoustic transducers shows potential for biomimetic sensor systems for measurements in a wide range of environmental conditions. The low power consumption of the miniaturized instrumentation offers new opportunities for portable biosensors dedicated to environmental analyses.[17]

Received: August 23, 2007
Published online: October 29, 2007

**Keywords:** biosensors · membranes · molecular recognition · piezoelectrics · polymerization

[1] S. D. Richardson, *Anal. Chem.* **2007**, *79*, 4295–4324.
[2] U.-B. Cheah, R. C. Kirkwood, K.-Y. Lum, *Pestic. Sci.* **1997**, *50*, 53–63.
[3] G. Vlatakis, L. I. Andersson, R. Muller, K. Mosbach, *Nature* **1993**, *361*, 645–647.
[4] F. Vandevelde, T. Leïchlé, C. Ayela, C. Bergaud, L. Nicu, K. Haupt, *Langmuir* **2007**, *23*, 6490–6493.
[5] F. L. Dickert, P. Forth, P. Lieberzeit, M. Tortschanoff, *Fresenius J. Anal. Chem.* **1998**, *360*, 759–762.

  

[6] K. Haupt, K. Noworyta, W. Kutner, *Anal. Commun.* **1999**, *36*, 391 – 393.
[7] K. Haupt, K. Mosbach, *Chem. Rev.* **2000**, *100*, 2495 – 2504; K. Lettau, A. Warsinke, M. Katterle, B. Danielsson, F. W. Scheller, *Angew. Chem.* **2006**, *118*, 7142 – 7146; *Angew. Chem. Int. Ed.* **2006**, *45*, 6986 – 6990.
[8] S. A. Piletsky, S. Subrahmanyam, A. P. F. Turner, *Sens. Rev.* **2001**, *21*, 2092 – 296.
[9] S. C. Huang, G. B. Lee, F. C. Chien, S. J. Chen, W. J. Chen, M. C. Yang, *J. Micromech. Microeng.* **2006**, *16*, 1251 – 1257.
[10] A. C. R. Grayson, R. S. Shawgo, A. M. Johnson, N. T. Flynn, L. Yamen, M. J. Cima, R. Langer, *Proc. IEEE* **2004**, *92*, 6 – 21.
[11] R. McKendry, J. Zhang, Y. Arntz, T. Strunz, M. Hegner, H. P. Lang, M. K. Baller, U. Certa, E. Meyer, H.-J. Güntherodt, C. Gerber, *Proc. Natl. Acad. Sci. USA* **2002**, *99*, 9783 – 9788; T. P. Burg, M. Godin, S. M. Knudsen, W. Shen, G. Carlson, J. S. Foster, K. Babcock, S. R. Manalis, *Nature* **2007**, *446*, 1066 – 1069.
[12] C. Ayela, L. Nicu, *Sens. Actuators B* **2007**, *123*, 860 – 868.
[13] M. Guirardel, L. Nicu, D. Saya, Y. Tauran, E. Cattan, D. Remiens, C. Bergaud, *Jpn. J. Appl. Phys.* **2003**, *43*, L111 – L114.
[14] K. Haupt, A. Dzgoev, K. Mosbach, *Anal. Chem.* **1998**, *70*, 628 – 631.
[15] M. Jakusch, M. Janotta, B. Mizaikoff, K. Mosbach, K. Haupt, *Anal. Chem.* **1999**, *71*, 4786 – 4791.
[16] R. H. Schmidt, A.-S. Belmont, K. Haupt, *Anal. Chim. Acta* **2005**, *542*, 118 – 124.
[17] Details about the experimental procedures employed in this paper are available in the Supporting Information.

  